npj | parkinson's disease

Article

Published in partnership with the Parkinson's Foundation

https://doi.org/10.1038/s41531-024-00865-1

Plasma fibronectin is a prognostic biomarker of disability in Parkinson's disease: a prospective, multicenter cohort study

Shuzhen Zhu[1,14], Hualin Li[1,14], Zifeng Huang[1,14], Yiheng Zeng[1,14], Jianmin Huang[1], Guixia Li[1], Shujuan Yang[1], Hang Zhou[1], Zihan Chang[1], Zhenchao Xie[1], Rongfang Que[1], Xiaobo Wei[1], Minzi Li[1], Yanran Liang[2], Wenbiao Xian[3], Mengyan Li[4], Ying Pan[5], Fanheng Huang[6], Lin Shi[7], Chengwu Yang[8], Chao Deng[9], Lucia Batzu[10], Karolina Poplawska-Domaszewicz[10], Shuhan Chen[11], Ling-Ling Chan[12,13], K Ray Chaudhuri[10] ✉, Eng-King Tan[12,13] ✉ & Qing Wang[1] ✉

In a prospective longitudinal study with 218 Parkinson's disease (PD) patients in the discovery cohort and 84 in the validation cohort, we aimed to identify novel blood biomarkers predicting disability milestones in PD. Through Least Absolute Shrinkage and Selection Operator-Cox (Lasso-Cox) regression, developed nomogram predictive model and Linear mixed-effects models, we identified low level of plasma fibronectin (pFN) as one of the best-performing risk markers in predicting disability milestones. A low level of pFN was associated with a short milestone-free survival period in PD. Longitudinal analysis showed an annual decline in the rate of pFN was significantly associated with the annual elevation rate in the Hoehn-Yahr stage. Moreover, pFN level was negatively correlated with phosphorylated α-synuclein, and a low level of pFN was associated with BBB disruption in the striatum on neuroimaging, providing evidence for pFN's role in PD progression. We finally identified pFN as a novel blood biomarker that predicted first-milestone disability in PD.

Parkinson's disease (PD) is one of the most common neurodegenerative disorders with an age-adjusted prevalence of 1.8%[1]. The progressive loss of dopaminergic neurons ultimately leads to disability 'milestones', such as recurrent falls, wheelchair dependence, residential home admission, hallucinations, dementia, and mortality for a large proportion of PD patients[2–5]. Those with disability milestones usually have poorer prognosis, a survival period of less than 5 years, and will exact a high financial cost for patients, their families, and the healthcare system[2,3,6,7].

However, among PD patients, there is marked heterogeneity in the rate of progression[4,8], which makes prognostication difficult and creates barriers for clinical trials aimed at delaying disability milestones[9]. As a consequence, prognostic biomarkers for milestones in PD are urgently needed,

[1]Department of Neurology, Zhujiang Hospital of Southern Medical University, Guangzhou, Guangdong, 510282, People's Republic of China. [2]Department of Neurology, Sun Yat-Sen Memorial Hospital of Sun Yat-sen University, Guangzhou, Guangdong, People's Republic of China. [3]Department of Neurology, The First Affiliated Hospital of Sun Yat-sen University, Guangzhou, Guangdong, People's Republic of China. [4]Department of Neurology, Guangzhou First People's Hospital of South China University of Technology, Guangzhou, Guangdong, People's Republic of China. [5]Department of Neurology, The Second Affiliated Hospital of Guangzhou Medical University, Guangzhou, Guangdong, People's Republic of China. [6]Department of Radiology, Zhujiang Hospital of Southern Medical University, Guangzhou, Guangdong, 510282, People's Republic of China. [7]Department of Imaging and Interventional Radiology, The Chinese University of Hong Kong, Hong Kong, Hong Kong SAR, People's Republic of China. [8]Division of Biostatistics and Health Services Research, Department of MassachusettPopulation and Quantitative Health Sciences, T.H. Chan School of Medicine, UMass Chan Medical School, Worcester, MA, 01605, USA. [9]School of Medical, Indigenous and Health Sciences, and Molecular Horizons, University of Wollongong, Wollongong, NSW, Australia. [10]Parkinson Foundation International Centre of Excellence at King's College Hospital, and Kings College, Denmark Hill, London, SE5 9RS, UK. [11]Guangdong Experimental High School, Guangzhou, Guangdong, 51000, People's Republic of China. [12]Department of Neurology, Singapore General Hospital, Singapore, Singapore. [13]Duke-National University of Singapore Medical School, Singapore, Singapore. [14]These authors contributed equally: Shuzhen Zhu, Hualin Li, Zifeng Huang, Yiheng Zeng.
✉e-mail: ray.chaudhuri@kcl.ac.uk; tan.eng.king@singhealth.com.sg; wqdennis@hotmail.com; denniswq@yahoo.com

particularly ones that could also dynamically monitor PD progression trajectory and ongoing pathological process[10,11].

To date, such biomarkers, especially for predicting milestones, are sparse. Current studies often focus on prognostic biomarkers for predicting motor or cognition decline in PD[9,12–15]. For example, Zhang et al. found cerebrospinal fluid (CSF) phosphorylated tau to total tau ratio and phosphorylated tau to Aβ42 ratio significantly correlated with the rate of change in motor Unified Parkinson's Disease Rating Scale (UPDRS)[9]. Compta et al. reported that lower baseline CSF concentrations of Aβ42 might predict cognitive decline[14]. Wang and Aarsland found that high levels of total plasma α-synuclein, neurofilament protein L(NfL), and lower epidermal growth factor predicted cognitive decline in PD[16].

Current studies have several limitations. First, the vast majority of the prognostic biomarkers predict motor or cognitive decline rather than disability 'milestones', which better reflect poor prognosis and have significant clinical relevance for late-stage PD[17–21]. Second, markers of peripheral inflammation, have not been evaluated for their clinical links with milestones in PD. Studies of these milestones, together with other biomarkers, have not been carried out using a prediction model[22–24]. Last, there are limited longitudinal studies that attempt to correlate pathological mechanisms with peripheral inflammation biomarkers[25].

To address these gaps in knowledge, we conducted a prospective multicohort study using a two-stage, discovery-validation design. We screened 19 blood-based peripheral inflammation biomarkers based on four major mechanisms: metabolic inflammation, coagulation molecules disorder, inflammatory immune cell imbalance, and increased inflammatory molecules in 218 longitudinally-followed PD patients. From these initial data, we identified plasma fibronectin (pFN) as the best-performing biomarker, which was then tested in a separate cohort with 84 longitudinally-followed PD patients. This validated pFN's ability to predict the onset of first-episode milestones and to monitor disease trajectory. Finally, we conducted functional studies by measuring the blood phosphorylated α-synuclein and neuroimaging studies to examine striatal blood–brain barrier (BBB) permeability to further characterize the relationship between plasma fibronectin and PD pathophysiologic changes.

Results

Overview of study design

A total of 19 blood markers, as well as 5 clinical variables based on peripheral inflammation-related mechanisms as previously reported, were selected as candidate prognostic markers. 5 clinical variables included age at onset, biological sex, disease duration, hypertension, and diabetes mellitus. 19 blood markers included hypersensitive C-reactive protein (HsCRP), lymphocyte, neutrophils, lymphocyte/neutrophils(L/N) ratio, uric acid (UA), cholesterol (Chol), high-density lipoprotein cholesterol (HDL-C), low-density lipoprotein cholesterol (LDL-C), fasting glucose (Glu), albumin (Alb), albumin/globulin ratio (A/G ratio), adenosine deaminase (ADA), retinol-binding protein (RBP), superoxide dismutase (SOD), lactate dehydrogenase (LDH), plasma fibronectin (pFN), fibrinogen (FIB), D-dimer (DDI) and plasminogen (PLG). Basis for the selection of candidate biomarkers is shown in Supplementary Table 1). PD patients with any of the six milestones, including recurrent falls, wheelchair dependence, residential home admission, severe hallucinations, dementia, and death, were defined as having a poor prognosis (Supplementary Table 2). We further assigned PD individuals into aggressive, mild, or N/A (information for grouping is not available due to insufficient follow-up period) subgroups based on the pace of progression to milestones. The aggressive clinical subtype refers to patients who suffered their first milestone <5 years after disease onset. The mild clinical subtype refers to those who developed their first milestone ≥5 years after disease onset. The N/A subtype refers to the remaining participants whose grouping information was not available (N/A) due to the fact that their disease course was less than 5 years, and no milestone was reached at the end of follow-up. These criteria of clinical subgroups were based on the longitudinal cohort studies of disease progression published by Hely and Lees[4].

We then (1) developed a prediction model with Least Absolute Shrinkage and Selection Operator-Cox (LASSO-COX) regression with blood inflammatory molecules as candidate markers to identify the best-performing biomarker at predicting the first-episode of milestones; (2) determined the association between the best-performing biomarker and the milestone-free survival period in the discovery cohorts and validated the initial result in a validation cohort; (3) investigated the correlation between the dynamic longitudinal change of the best-performing biomarker level and disease progression trajectory in three clinical subtypes (aggressive, mild and N/A) and; (4) analyzed the correlation between the best-performing biomarker and α-synuclein, blood–brain barrier (BBB) permeability, as well as and the correlation between the levels of the best-performing biomarker in the peripheral blood and CSF to explore the underlying pathophysiological mechanisms of the best-performing biomarker on disease progression. The overview of the study design is shown in Fig. 1.

Cohorts and sample collection

A total of 392 clinically screened PD participants without disability milestones at the time of the initial visit and with magnetic resonance imaging (MRI) scans between December 2011 and November 2021 through 5 hospitals of the South China Parkinson's Disease Alliance were included in the analysis. All individuals met the diagnostic criteria of the 2015 Movement Disorder Society[26]. After screening by the inclusion and exclusion criteria (shown in supplemental data page 1), 302 eligible subjects were enrolled, and then assigned to two cohorts: discovery and validation. This is a two-stage study. The discovery cohort is a retrospective cohort study, while the validation cohort is a prospective validation cohort. Because there is a discovery cohort in Oxford England who have published[27], here we call our discovery cohort as Discovery-C cohort (c for China). The study was approved by the ethics committee at Zhujiang Hospital of Southern Medical in Guangzhou (Project number 2021-KY-023-01, Clinical trial registration no. ChiCTR2100045714). The study flowchart is detailed in Supplementary Fig. 1. Demographics and baseline clinical parameters in these two cohorts were summarized in Table 1.

The Discovery-C cohort consisted of a total of 218 participants who were enrolled from December 2011 to March 2021 at Zhujiang Hospital of Southern Medical University (ZJH_SMU, $n = 196$), Guangzhou First People's Hospital of South China University of Technology (GZF_SCUT, $n = 15$) and the First Affiliated Hospital of Sun Yat-sen University (FH_SYS, $n = 7$) and received a retrospective investigation were assigned to the discovery cohort. All individuals had baseline clinical variables collection, such as UPDRS, MMSE, MoCA, Levodopa Equivalent Daily Dose (LEDD), Hoehn and Yahr (H&Y) stage, and results of peripheral inflammation-related blood markers. Among them, 20 individuals had CSF sampling at the baseline time point. All individuals were followed at variable intervals, and the milestones-free period was recorded after follow-up. Among them, 96 individuals had longitudinally repeated collection of the following: Levodopa Equivalent Daily Dose (LEDD), Hoehn and Yahr (H&Y) stage, and blood samples. The interval between two follow-up visits ranges from once a month to once every 6 months. The frequency of follow-up visits is between 2 and 7 times. The maximum follow-up time for the discovery cohort is 72 months (interquartile range [IQR] is 10.29–36.08 months, with a median follow-up of 26.6 months). The ZJH_SMU institutional review board approved study protocols, and all participants consented to the study.

The validation cohort consisted of a total of 84 PD patients who were enrolled from October 2020 to November 2021 at Zhujiang Hospital of Southern Medical University (ZJH_SMU, $n = 80$), Sun Yat-sen Memorial Hospital of Sun Yat-sen University (MH_SYS, $n = 3$), the Second Affiliated Hospital of Guangzhou Medical University (SH_GMU, $n = 1$) were assigned to the validation cohort. 72 individuals had a DCE-MRI scan, and 23 individuals had plasma alpha-synuclein testing at baseline time point. A prospective follow-up was conducted every 3.0 months. The maximum follow-up time for the validation cohort is 17.0 months (interquartile range [IQR] is 2.0–11.0 months, with a median follow-up of 5.0 months). The milestones-free period was recorded after follow-up.

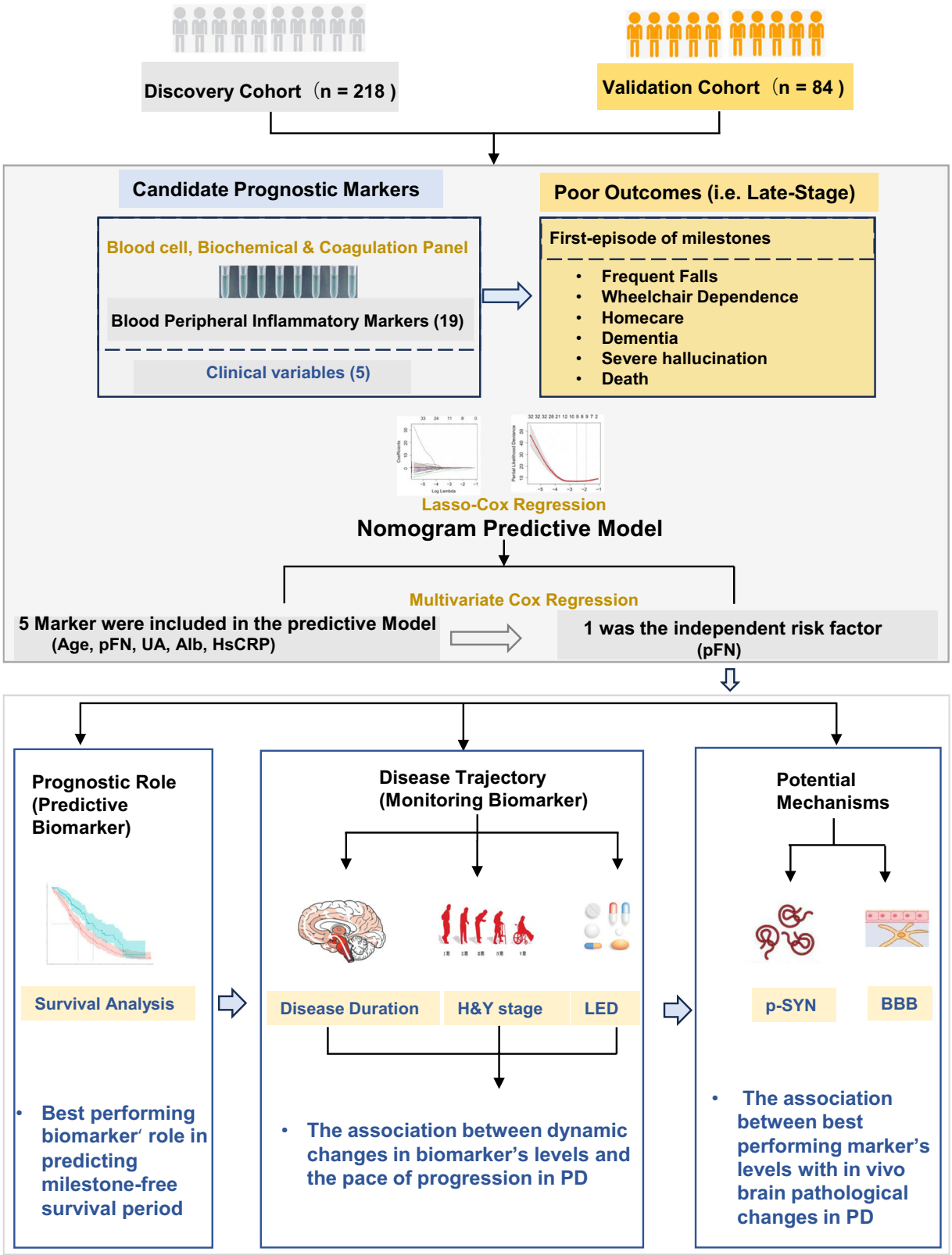

Fig. 1 | Study overview. 302 PD participants were assigned to the Discovery Cohort ($n = 218$, left panel) and Validation Cohort ($n = 84$, right panel). A Lasso-Cox regression was used to screen the best-performing marker out of 19 peripheral inflammation blood markers to predicate the duration of disability milestone-free survival. Next, with longitudinal data, LMEMs were used to correlate the annual change of this best-performing marker with disease progression as assessed by the annual change of H&Y stage and LED. Finally, we measured BBB permeability in the striatum and the level of α-synuclein in the blood to explore the potential mechanisms of the best-performing biomarker in promoting PD progression to milestones. BBB blood–brain barrier, H&Y Hoehn-Yahr, LED equivalent doses of levodopa, LMEMs linear mixed-effects models.

Table 1 | Participant characteristics in discovery and validation cohorts

Characteristic	Discovery cohort (*n* = 218)	Validation cohort (*n* = 84)	*p*-value
Demographic			
Median age at onset, years	63 (54–68)	64 (58.5–69.5)	0.094
Sex, no. (%)			
Male	129 (59.18%)	52 (61.90%)	0.003**
Baseline clinical status			
Disease duration, median (95% CI), years[a]	4 (2–6)	3 (2–6)	0.612
Comorbidity			
DM, no. (%)	7 (3.21%)	6 (7.14%)	0.201[a]
HBP, no. (%)	44 (20.18%)	29 (34.52%)	0.009**
H&Y stage	3.5 (2–4)	4 (3–4)	0.001**
UPDRS (total)	42.5 (29.0–76.2)	48.0 (33.6–60.8)	0.616
UPDRS I	2 (0.75–2)	4 (3–5)	<0.001***
UPDRS II	12 (5–18)	12 (8–16)	0.193
UPDRS III	23 (16–56)	27 (18–36)	0.642
UPDRS IV	5 (2–7)	5 (3–7)	0.198
MMSE	25 (23–28)	26.5 (23–29)	0.383
MOCA	19 (15–25)	21 (16–23)	0.209
LED (mg)	500 (375–673)	611 (474–799)	<0.001***
Baseline laboratory test			
HsCRP, mg/L	0.5 (0–0.82)	0 (0–0.59)	<0.001
Lymphocyte, G/L	1.82 (1.50–2.32)	1.90 (1.64–2.21)	0.488
Neutrophils, G/L	3.55 (2.79–4.25)	3.64 (2.98–4.41)	0.336
L/N ratio,	0.55 (0.40–0.70)	0.53 (0.40–0.67)	0.815
UA, μmol/L	316 (263–378)	316 (269–375)	0.840
Chol, mmol/L	4.48 (3.89–5.10)	4.36 (3.74–4.99)	0.304
HDL-C, mmol/L	1.54 (1.26–5.01)	1.26 (1.05–1.44)	<0.001***
LDL-C, mmol/L	2.69 (2.16–3.34)	2.61 (2.17–3.30)	0.829
Glu, mmol/L	4.74 (4.44–5.18)	4.92 (4.58–5.31)	0.045*
Alb, g/L	39.8 (37.5–42.0)	40.4 (38.75–42.35)	0.273
A/G ratio	1.50 (1.30–1.60)	1.60 (1.40–1.75)	0.023*
ADA, IU/L	8.30 (7.01–10.09)	8.52 (7.31–10.58)	0.641
RBP, mg/L	40.80 (34.50–48.30)	41.95 (36.65–47.95)	0.354
SOD, kU/L	139 (125–155)	152 (142–165.5)	<0.001***
LDH, IU/L	168.0 (149.7–189.6)	176.8 (153.8–187.0)	0.252
FIB, g/L	3.05 (2.61–3.35)	2.69 (2.27–2.97)	<0.001***
DDI, mg/L	0.39 (0.27–0.65)	0.39 (0.2–0.66)	0.220
PLG, %	95 (85.0–106.0)	91.3 (84.6–100.55)	0.129
pFN, mg/L	200.1 (182.7–227.0)	206.0 (181.0–231.0)	0.438
Milestones			
First-episode of milestone			
Events	77 (35.32%)	28 (33.33%)	0.745
Median time since initial diagnosis, years	4.13 (2.08–7.14)	5.50 (3.02–7.90)	0.373
Frequent Falls			
Events	45 (20.64%)	7 (8.33%)	<0.001***
Median time since initial diagnosis, years	6.46 (4.17–9.50)	5.33 (3.33–7.33)	0.332
Wheelchair dependence			
Events	21 (9.63%)	9 (10.71%)	0.128
Median time since initial diagnosis, years	7.25 (5.75–11.75)	5.00 (3.08–8.46)	0.025
Home care			
Events	30 (13.76%)	10 (11.90%)	0.670
Median time since initial diagnosis, years	7.13 (3.92–12.27)	7.83 (3.00–9.60)	0.724
Dementia			
Events	19 (8.72%)	7 (8.33%)	0.915
Median time since initial diagnosis, years	5.75 (3.17–8.50)	3.08 (1.92–7.00)	0.306
Severe Hallucination			
Events	14 (6.42%)	1(1.19%)	0.076[a]
Median time since initial diagnosis, years	4.08 (3.02–8.71)	NA	0.533
Death			
Events	5 (2.29%)	1 (1.19%)	0.682
Median time since initial diagnosis, years	4.33 (3.54–9.88)	NA	0.667
Cause of death			
PD-related events	3 (1.38%)	1 (1.19%)	1.000
PD-unrelated events	2 (0.92%)	0	

ADA adenosine deaminase, *Alb* albumin, *A/G* ratio, *Chol* cholesterol, *DDI* D-dimer, *DM* diabetes mellitus, *FIB* fibrinogen, *Glu* glucose, *HBP* high blood pressure, *HDL-C* high-density lipoprotein cholesterol, *HsCRP* hypersensitive C-reactive protein, *H&Y* Hoehn-Yahr, *LDH* lactate dehydrogenase, *LDL-C* Low-density lipoprotein cholesterol, *LED* levo-dopa-equivalence dosage, *L/N* ratio, lymphocyte/neutrophils ratio, *MMSE* mini-mental state examination, *MOCA* Montreal cognitive assessment, *NA* non-available, *pFN* plasma fibronectin, *PLG* plasminogen, *RBP* retinol-binding protein, *SOD* superoxide dismutase, *UA* uric acid, *UPDRS* unified Parkinson's disease rating scale.

*$p < 0.05$; **$p < 0.01$; ***$p < 0.001$.

[a]Fisher's Exact test.

Age, pFN, UA, Alb, and HsCRP were selected for the nomogram predictive model analysis

To study the role of peripheral inflammation in predicting the progression of PD, the LASSO-COX method was used to construct a prediction model to identify valuable prognostic biomarkers. The predictors in the model included age at onset, plasma fibronectin (pFN), uric acid (UA), albumin (Alb), and hypersensitive C-reactive protein (HsCRP). The coefficients were 0.024246 (age), −0.017086 (pFN), -0.001545 (UA), −0.068079 (Alb), and 0.016296 (hsCRP) (Supplementary Fig. 2A, B). According to the calibration plots, the model's predicted probabilities were close to the observed probabilities (Fig. 2a–c). The nomogram based on the overall prediction model is shown in Fig. 2d, and the estimated 1-year, 3-year, and 5-year survival probabilities generated by the nomogram are shown in Supplementary Table 3. A receiver operating characteristic (ROC) curve was used to determine the optimal cutoff value. The optimal threshold value was defined as the final cutoff value in univariate Cox regression analysis. The cutoff values of the predictive factors age, pFN, UA, Alb, and hsCRP were 54 y, 197.6 mg/L, 306 μmol/L, 37.8 g, and 2.1 mg/L, respectively. The C-index of the prediction model was 0.705. The cutoff values were defined with the

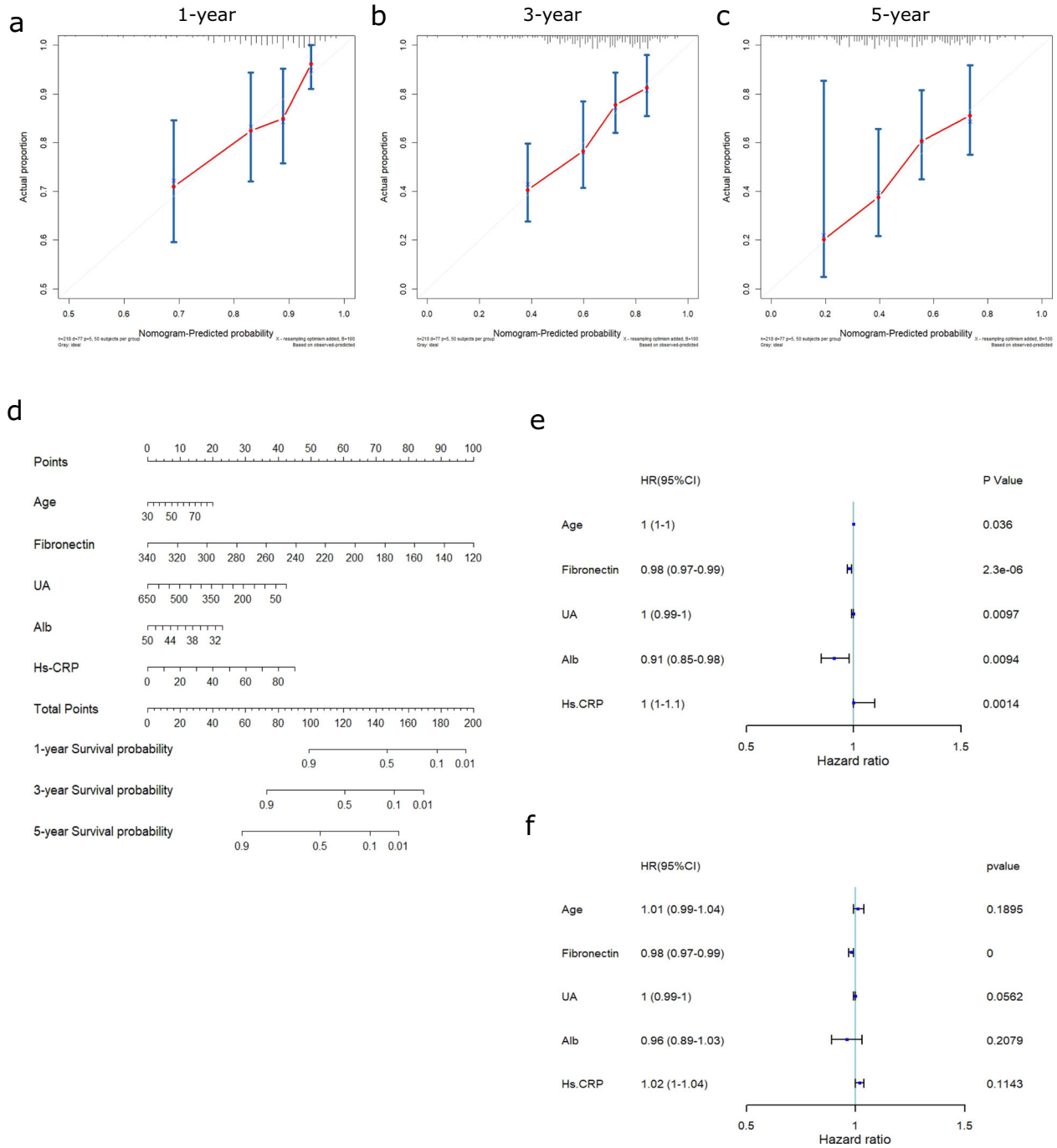

Fig. 2 | pFN is an independent risk factor for poor clinical prognosis as assessed by Cox regression. a–c Calibration plots of overall survival probabilities at 1 year (**a**), 3 years (**b**), and 5 years (**c**). Nomogram-predicted overall survival is plotted on the *x*-axis, with observed overall survival on the *y*-axis. Dashed lines along the diagonal line through the origin point represent the perfect calibration models in which the predicted probabilities are identical to the observed probabilities. **d** Nomogram for predicting the probability of overall survival at 1 year, 3 years, and 5 years. The number of points for each clinical characteristic is shown in the top row. For each characteristic, absence is assigned 0 points. The presence of characteristics is associated with a number of points generated using the nomogram function, Svy-Nom package in R, based on the results of LASSO analysis. The points for each characteristic are summed together to generate a total-point score. **e**, **f** Forest plots were generated to visualize the association between the abovementioned predictors and overall survival by univariate (**e**) and multivariate Cox regression analyses (**f**). The cutoffs used in univariate Cox regression for age, pFN, UA, Alb, and hsCRP were 54 y, 197.6 mg/L, 306 μmol/L, 37.8 g, and 2.1 mg/L, respectively. The C-index of the survival model was 0.705. Alb albumin, HR hazard ratio, hsCRP hypersensitive C-reactive protein, pFN plasma fibronectin, UA uric acid.

enumeration method in Supplementary Fig. 3, and the ROC analysis graphs were shown in Supplementary Fig. 4. In addition, we compared the HsCRP, Alb, UA, and pFN levels of 218 individuals in the discovery cohort with sex- and age-matched control groups. The results showed that there was only a statistical difference between the two groups at the levels of HsCRP and pFN (Supplementary Table 4).

Plasma protein pFN is an independent risk factor and best-performing marker for first-episode of milestones

To determine which biomarkers served as independent predictors in the nomogram model, a forest plot was generated to visualize the association between the predictors and milestone-free survival period with univariate and multivariate Cox regression analyses (Fig. 2e, f) and Table 2. According

Table 2 | Multivariate analysis (crude and adjusted) of predictors selected by LASSO regression procedure in the discovery cohort (first milestone)

	Definition	Univariate Cox regression		Multivariate Cox regression	
		Crude HR (95% CI)	*p*-value	Adjusted HR (95% CI)	*p*-value
First milestone					
pFN	mg/dL	0.981 (0.973–0.989)	<0.001***	0.982 (0.974–0.99)	<0.001***
Age	years	1.023 (1.001–1.045)	0.040*	1.014 (0.993–1.036)	0.198
UA	μmol/L	0.997 (0.994–0.999)	0.019*	0.998 (0.995–1)	0.096
Alb	g/L	0.912 (0.852–0.977)	0.009**	0.954 (0.889–1.024)	0.194
HsCRP	mg/L	1.037 (1.014–1.060)	0.001**	1.019 (0.995–1.044)	0.115

HR hazard ratio, *HsCRP* hypersensitive C-reactive protein, *UA* uric acid, *Alb* albumin, *pFN* plasma fibronectin.
*$p < 0.05$; **$p < 0.01$; ***$p < 0.001$.

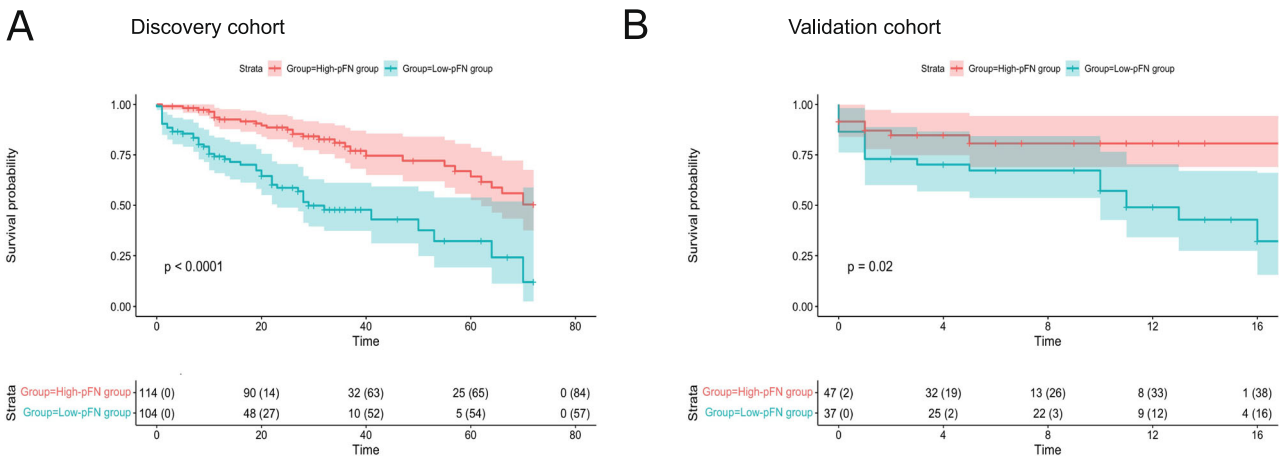

Fig. 3 | Predicting disease progression by baseline pFN as assessed by first milestone-free survival analysis. a, **b** first milestone-free survival curves for the discovery cohort (**a**) and validation cohort (**b**), stratified into low-pFN and high-pFN groups according to an optimal cutoff point of 197.6 mg/L. pFN plasma fibronectin.

to univariate Cox regression, the HR (95% CI, *p*) of age was 1 (1–1, $p = 0.036$), the HR of pFN was 0.98 (0.97–0.99, $p < 0.0001$), the HR of UA was 1 (0.99–1, $p = 0.0097$), the HR of Alb was 0.91 (0.85–0.98, $p = 0.0094$), and the HR of hsCRP was 1 (1–1, $p = 0.0014$). According to multivariate Cox regression analysis, the HR (95% CI, *p*) of age was 1.01 (0.99–1.04, $p = 0.1894$), that of pFN was 0.98 (0.97-0.99, $p < 0.0001$), that of UA was 1 (0.99-1, $p = 0.0562$), that of Alb was 0.96 (0.89–1.03, $p = 0.2079$) and that of hsCRP was 1.02 (1–1.04, $p = 0.1143$). Multivariate analysis showed that pFN was the only independent risk factor for predicting prognosis in our model ($p < 0.001$). The multivariate analysis (crude and adjusted) of predictors selected by the LASSO regression procedure for other milestones (all) was also shown in Supplementary Table 5.

Low level of pFN is associated with a short milestone-free survival period in PD

Kaplan–Meier curves of the cumulative risk of milestones were generated to explore the impact of pFN level on milestone-free survival duration in PD patients. All participants were stratified into two groups (high pFN ≥197.6 mg/L vs. low pFN <197.6 mg/L) using the calculated optimal pFN cutoff value. The results showed that the median milestone-free survival time (from diagnosis to the onset of milestones) for low-pFN patients (high-risk) versus high-pFN patients (low-risk) was 7.05 years (95% CI 6.022–8.075) versus 11.22 years (9.745–12.695; $\chi^2 = 7.913$, $p < 0.005$; Table 1) in the discovery cohort, 7.833 years (4.869–10.798) versus 10.250 years (8.580–11.920; $\chi^2 = 2.254$, $p = 0.133$; Table 1) in the validation cohort. The median milestone-free survival time (from baseline visit to the onset of milestones) for high-pFN patients versus low-pFN patients was 57.179 months (95% CI 52.495–61.863) versus 37.168 months (30.781–43.628; $\chi^2 = 27.069$, $p < 0.0001$; Fig. 3a) in the discovery cohort, 14.249 months (12.05–12.900) versus 10.249 months (7.913–12.585; $\chi^2 = 5.455$, $p = 0.02$; Fig. 3b) in the validation cohort. Our results demonstrate that pFN is a prognostic biomarker for predicting disability milestones in PD patients. Apart from the first-milestone episode, we also analyzed the impact of baseline pFN levels on the rate of progress to the development of each milestone, as shown in Supplementary Fig. 5.

pFN levels correlate with rate of progression in PD

Given that baseline pFN is a potential prognostic biomarker, we further explored whether dynamic changes in pFN levels could reflect the pace of progression in PD and be used to monitor disease progression. We first analyzed the data from the discovery cohort. Among the 218 participants, 96 (32%) returned for at least 1 and at most 6 follow-up visits, with a mean number of 1.89 (95% CI 1.62–2.17) visits and a median observation time of 5.5 years (IQR 3.5–8.0) from the baseline visit. All participants were divided into 3 clinical subtypes (aggressive, mild, and N/A). Here, the "N/A" group was not included in the analysis. The estimated annual changes in pFN showed that compared with the mild group, the annual decline in pFN was more rapid in the aggressive group within 5 years after onset. Longitudinal pFN distinguished aggressive from mild subtypes as evaluated by multivariate linear mixed-effects models (LMEMs) (b (2.5%, 97.5%) = −0.07 (−0.14, −0.01), $p = 0.03$, Fig. 4a).

To identify whether annual pFN change reflects disease progression as assessed by Hoehn-Yahr (H&Y) stage, the correlation between baseline pFN and the annual change in pFN, between the annual change in pFN and the annual change in (H&Y) stage was analyzed using LMEMs. The results showed no significant association between the baseline pFN and the annual

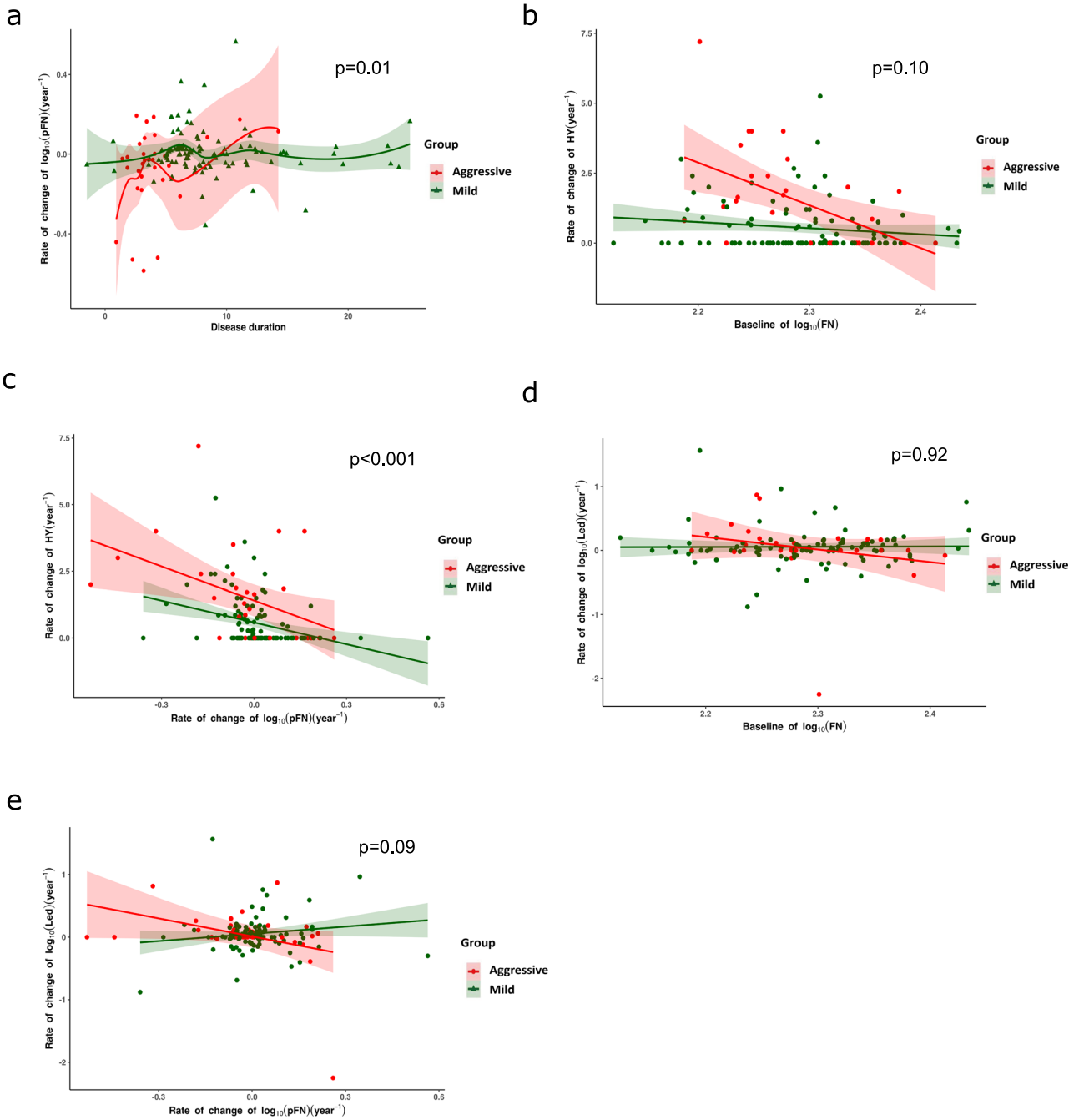

Fig. 4 | Monitoring disease progression by baseline pFN and pFN rate of change. **a** Estimated annual change in pFN based on disease course in patients. Colored symbols represent the individual random effect slope estimates. The shaded areas represent the 99% credible intervals. Longitudinal pFN distinguishes aggressive from mild very early (before 5 years of disease progress) as evaluated by multivariate linear mixed-effects models (LMEMs) (**b** (2.5%, 97.5%) = −0.07 (−0.14, −0.01), $p = 0.03$). **b** Prediction of changes in Hoehn-Yahr stage by baseline pFN. Lower baseline pFN levels were significantly associated with an increased rate of change in the elevation of clinical Hoehn-Yahr stage in the aggressive group ($n = 11$; **b** (2.5%, 97.5%) = 29.53 (12.55–46.50), $p < 0.001$), but no association was found in the mild group ($n = 56$; **b** (2.5%, 97.5%) = −2.42 (−5.69 to 0.85), $p = 0.15$). **c** Rate of change of plasma FN per year in the aggressive subtype mirrors the rate of change in the Hoehn-Yahr stage. LMEMs were used to evaluate the correlation between these two variables, and the shaded area around each linear fit line represents the quantile (2.5% to 97.5%). A significant association between rate of change of pFN and Hoehn-Yahr score was noted in both the aggressive group and the mild group (aggressive: $n = 11$, visit time = 28; **b** (2.5%, 97.5%) = 0.84 (0.43, 1.24), $p < 0.001$; mild: $n = 56$; visit time = 115, **b** (2.5%, 97.5%) = −2.65 (−4.36, 0.95), $p < 0.001$). **d** The role of baseline pFN in predicting the changes in LED. Lower baseline pFN levels were not significantly associated with an increased rate of change in LED elevation in the aggressive group ($n = 11$; **b** (2.5%, 97.5%) = 4.42 (−1.48,10.32), $p = 0.13$), mild group ($n = 56$; **b** (2.5%, 97.5%) = 0.02 (−1.12,1.15), $p = 0.98$)). **e** The role of rate of change in plasma FN per year in predicting the changes in LED. Using LMEMs, no association was found in any group (aggressive: $n = 11$; **b** (2.5%, 97.5%) = −0.03 (−0.18,0.10), $p = 0.62$; mild: $n = 56$; **b** (2.5% to 97.5%) = 0.42 (−0.15, 0.99), $p = 0.15$).

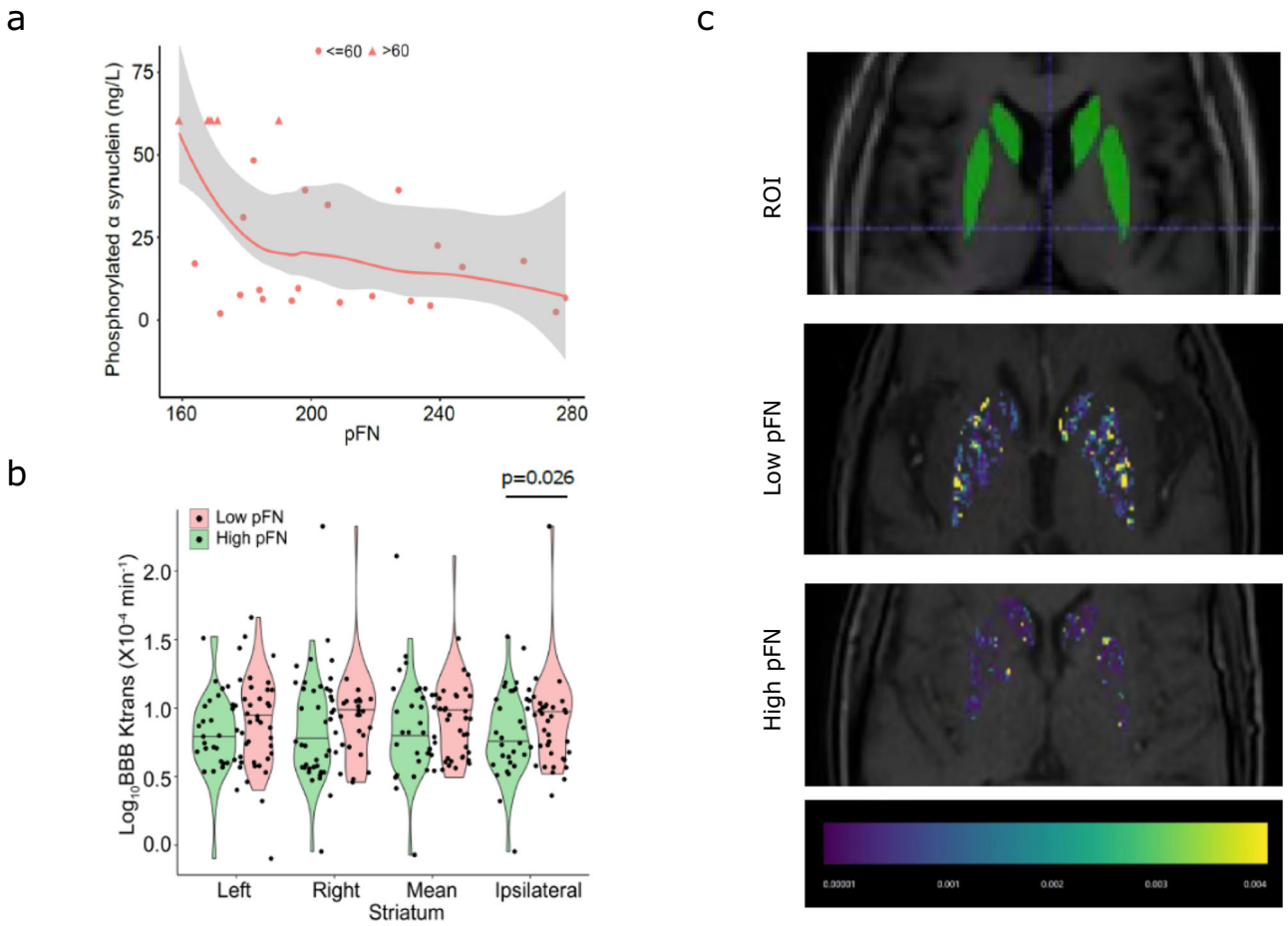

Fig. 5 | Correlations between baseline pFN and phosphorylated α-synuclein, and baseline pFN and blood–brain barrier permeability of the striatum. **a** Clinicopathologic correlation analysis revealed significant negative correlations between pFN and phosphorylated α synuclein (correlation coefficient, −0.456; $p = 0.008$) using the Spearman correlation test. **b** Comparison of K^{trans} values in the striatum between the high-FN group and the low-FN group (left, right, average, and ipsilateral). **c** Representative images of BBB permeability in the low-pFN group and the high-pFN group, as well as a localization marker image of the region of interest. The T1 sequence was used to localize the striatum.

change in H&Y stage (aggressive: **b** (2.5%, 97.5%) = 4.24 (−1.22, 9.69), $p = 0.13$; mild: $n = 56$; visit time = 115, **b** (2.5%, 97.5%) = −0.02 (−0.16, 1.03), $p = 0.98$;) (Fig. 4b). The results showed a significant association between the change rate of pFN and the annual change in H&Y stage in the aggressive group and the mild group (aggressive: $n = 11$, visit time = 28, **b** (2.5%, 97.5%) = 0.84 (0.43, 1.24), $p < 0.001$; mild: $n = 56$; visit time = 115, **b** (2.5%, 97.5%) = −2.65 (−4.36,0.95), $p < 0.001$ (Fig. 4c). These longitudinal analyses suggest that the dynamic changes in pFN can reflect the progression of PD.

To identify whether the annual pFN change reflects the change in levodopa equivalent dose (LED), the correlation between the annual change in pFN and the annual change in LED was also analyzed using LMEMs. The results showed no significant association between the change rate of pFN and the annual change in LED in the aggressive group or the mild group as showed in Fig. 4d, e. The statistical p-value of the difference in correlation of pFN with H&Y or LED between the two groups was also shown in the Fig. 4.

pFN levels correlate with in vivo brain pathological changes in PD

PD is characterized by the aggregation and extravasation of p-α-SYN[28,29]. To explore whether pFN was involved in the pathophysiologic progress of PD, we investigated the correlation between pFN and blood p-α-SYN levels. Interestingly, a biphasic monotonic function relationship between baseline pFN and plasma phosphorylated α-synuclein levels was observed. A significant negative correlation between pFN and p-α-SYN ($n = 26$, correlation coefficient = −0.456; $p = 0.008$) was observed with the Spearman correlation test. The simulation curve of the correlation between the two variables is shown in Fig. 5a, suggesting that a low baseline level of pFN may be associated with the aggregation of pathologic α-synuclein.

Peripheral inflammation can induce BBB disruption[30]. Due to the retrospective nature of the discovery cohort, baseline data of dynamic contrast-enhancement magnetic resonance imaging (DCE-MRI) were not available for the majority of PD patients. So, in this study, we only conducted DCE-MRI examination in individuals in the validation cohort. Results showed that in the validation cohort, 67 (79.76%) of 84 participants were eligible for BBB permeability evaluation using DCE-MRI. Seventeen (20.24%) of 84 patients were excluded for the following reasons: 11 had microinfarcts in the striatum, 4 had microbleeds in the striatum, and 2 had artifacts caused by severe head tremor. Among the 67 eligible participants, 33 of 67 were assigned to the low-pFN group, and 34 of 67 were assigned to the high-pFN group. The baseline data (sex, age and disease duration) between the low-pFN and high-pFN groups were compared, and no difference was found (Supplementary Table 6). The Mann–Whitney U test was used to compare the K^{trans} value in the striatum between the high-pFN and low-pFN groups. The median K^{trans} in the ipsilateral or relatively severe damaged striatum of high-pFN patients versus low-pFN patients was $5.39 \times 10^{-4}\,min^{-1}$ ($n = 34$, IQR 4.12–9.22) versus $9.91 \times 10^{-4}\,min^{-1}$ ($n = 33$, IQR 4.78–13.38; $p = 0.027$; Fig. 5b). Representative DCE-MRI images are

shown in Fig. 5c. This result suggests that low level of pFN is associated with increased BBB permeability in the striatum.

A positive correlation trend was observed between the levels of FN in the plasma and the CSF (Spearman correlation coefficient=0.547, $p = 0.028$) (Supplementary Fig. 6A), suggesting that the FN level in plasma could be used to indicate its level in CSF. After $\log_{10}$ transformation of FN, using a linear regression model, we found that the level of $\log_{10}$ FN in the CSF and the plasma was positively linearly correlated after adjusting for age, sex, and disease course ($F = 3.65$, $R^2 = 0.57$, adjusted $R^2 = 0.41$, $p = 0.04$) (Supplementary Fig. 6B). A correlation between pFN level in the blood and the CSF was found indicating that the changes in cerebrospinal fluid FN can partly be reflected by detecting the FN value in blood.

Taken together, these analyses suggest that pFN is a clinically useful prognostic biomarker that could potentially be used to predict disease prognosis, monitor disease progression, and reflect brain pathological changes.

Discussion

Our findings have potential clinical relevance as the identified pFN biomarker can be used to predict clinical prognosis, and be used as an outcome measure for clinical trials aimed at delaying or preventing the onset of disability milestones in PD. Inflammation plays a crucial role in the progression of PD[31–33]. Recent studies have suggested that markers of inflammation are involved in various pathophysiologic pathways in PD and are potential prognostic biomarkers for PD[34–37]. The vast majority of previous studies have mainly focused on the relationship between inflammatory cells or proteins and PD progression. However, apart from inflammatory cells and proteins, other biomarkers, including coagulation and metabolic molecules such as fibrinogen, ALB, UA, Chol, glucose, and HsCRP may also be associated with inflammation initiation and involved in disease progression[38]. For example, we previously found that lipoprotein cholesterol level was associated with motor severity of PD[39]. Chen-Plotkin et al. reported that plasma CRP and albumin levels may be predictive of the rate of cognitive change in PD[40]. High baseline levels of UA, CRP, high-density lipoprotein (HDL) cholesterol, and glucose levels were also identified as risk parameters for faster disease progression[41,42]. To address this gap, we selected 19 inflammatory markers that can be conveniently tested in clinical routine practice, including multiple inflammation-related mechanisms, such as inflammatory proteins, inflammatory cells, coagulation molecules, and metabolic molecules (such as glucose, proteins, cholesterol, and purine metabolism molecules), et al. Our study highlights a novel prognostic biomarker, that is, baseline plasma FN as a best-performing biomarker for predicting the rate of onset of milestones in PD individuals.

pFN is mainly secreted by liver cells and partly derived from intrathecal synthesis. The decrease in pFN levels has been proven to be positively related to acute and chronic inflammation[43,44] and poor clinical prognosis in individuals with a variable of diseases, such as sepsis[45]. The mechanisms by which inflammation leads to a decrease in pFN levels are currently not fully understood. The main viewpoint is that the decrease in pFN is related to the phagocytic activity of the reticuloendothelial system (RES). As early as 1981, Pott G et al. found that patients with sepsis and shock had a definite decrease of pFN during the course of the disease[46]. During inflammation, the phagocytic function of Reticuloendothelial function is activated. Due to its opsonizing role, pFN binds to circulating degradation products and mediates their elimination by the reticuloendothelial system, which leads to the depletion of pFN by RES[47]. Although pFN has been found to be associated with the prognosis of ischemic stroke and traumatic brain injury, there is little research on its role in PD. Recent research found that pFN enhanced the survival of transplanted neuron survival in nigral[48], supported neurite outgrowth and axonal regeneration of adult brain neurons[49], modulated microglia M1/M2 polarization, and alleviated pathologic alpha-synuclein accumulation in PD animal model[50]. In our study, we found that a dramatic decline of pFN, especially in about the first 9 years of onset, signified a faster disease progression and a more aggressive clinical subtype in PD, which is consistent with previous research. Based on the above findings, pFN might also be involved in the progression of PD, possibly through inflammatory modulation and/or neuroprotection.

The primary pathologic change of PD includes the misfolding and aggregation of α-syn, as well as the degeneration of dopaminergic neurons. Currently, limited research has been conducted in terms of the correlation between FN and synuclein. In 2023, Adulla, A. reported that alpha-Synuclein modulates fibronectin expression. In 2024, Dai W. et al. reported their results that the administration of pFN reduced the level of α-syn in the striatum in PD animal model[50]. In this study, we also found a negative relationship between pFN and phosphorylated α-synuclein. This result also implies that a low baseline pFN level may potentially be associated with the aggravation of the accumulation of pathologic α-synuclein.

During the progression of PD, the integrity of the BBB becomes compromised. However, the relationship between pFN and BBB was largely unknown. pFN was found to be related to human endothelial cell adhesion, cell spreading, and proliferation. Current research showed that pFN alleviated activation of astrocytes and aggregation of α-synuclein in the striatum. In our study, we also found that patients with low levels of pFN had higher striatal BBB permeability on neuroimaging studies, indicating that pFN levels could reflect pathological damage to the brain in PD patients and that low pFN might accelerate BBB permeability.

Our study has the following strengths: (1) we have included inflammatory biomarkers with multiple mechanisms in the analysis, through which novel biomarkers were identified; (2) we used disability milestones, and clinically relevant outcomes for more severe PD, and these served as prognostic endpoints rather than cognitive decline or motor progression; (3) we have used a discovery-validation two-stage study design; and (4) we conducted functional studies to determine the possible underlying mechanisms linking pFN with the onset of PD disability milestones.

Our study also has several limitations: (1) one limitation is that due to the retrospective nature of the discovery cohort, baseline data of DCE-MRI and p-α-syn data were not available for the majority of PD patients in this cohort; however, in the prospective validation cohort, the follow-up duration is relatively short compared to the discovery cohort, leading the median survival times in the validation cohort are more than 3 times of those in the discovery cohort. (2) the second limitation is that pFN mainly predicts time to the first event and motor problems (falls, wheelchair, home care), but not dementia, hallucinations, or death, suggesting that it is related to peripheral deterioration rather than CNS issues; (3) the third limitation is that just like in the real world, in our cohort, the majority of PD patients exhibits benign clinical course, with relatively fewer cases presenting a aggressive progression course; (4) The correlation coefficient between pFN and p-a-SYN was -0.456 ($p = 0.008$), indicating a weak correlation between these two indices and the values for p-α-synuclein are capped at 60 ng/mL due to the limitations of the detection range of the Elisa kit, leading to overall low confidence in the validity of this analysis.

In conclusion, we identified pFN as a novel blood biomarker that predicted first-milestone disability in PD and functional study revealed that pFN negatively correlated with phosphorylated α-synuclein. Our findings suggest that pFN can be used for disease monitoring and prognostication in clinical practice and trials in PD.

Methods

Ethical approval and consent to participate

The human biomarker and neuroimaging studies were approved by the ethics committee at Zhujiang Hospital of Southern Medical in Guangzhou (Project number 2021-KY-023-01, Clinical trial registration no. ChiCTR2100045714).

Clinical data

The rate of change in the H&Y stage or LED elevation was calculated using the H&Y score or LED difference between two adjacent follow-up visits divided by the duration of time (years) between the two visits.

Biomarker quantification

The selection and detection methods of candidate biomarkers are shown in Supplementary Table 4 in detail. Blood biomarker quantification was performed at Zhujiang Hospital of Southern Medical University. Fibronectin (FN) level in CSF samples was measured in Guangzhou Kingmed Center for Clinical Laboratory, Co., Ltd.

Peripheral venous blood was collected in the morning after fasting for 8 h using a BD Vacutainer (Becton Dickinson and Company, United Kingdom). Samples for blood cell count (lymphocyte and neutrophils) were collected with purple EDTA-K2 anticoagulant tubes. Samples for blood coagulation process monitoring were collected with blue top sodium citrate vacutainer tubes. Samples for serum assessment were collected with red top plain vacutainer tubes. Plasma samples for fibronectin assessment were collected with green sodium heparin 95 USP units in blood collection tubes. After blood collection, plasma and serum tubes were centrifuged at 2,000 × g for 15 min at room temperature. After centrifugation, the supernatant was collected with a disposable, nonsterile transfer pipette into a single transfer tube (SARSTEDT AG & Co. KG) and placed in a −80 °C refrigerator for later testing. Cerebrospinal fluid (CSF) was collected in polypropylene tubes after standard lumbar puncture procedures.

Plasma and CSF FN measurements were performed using a Human Fibronectin Enzyme-linked immunosorbent assay (ELISA) kit (ab108848 for plasma and ab108847 for CSF, Abcam, Cambridge, UK). Plasma phosphorylation alpha-synuclein was measured using the Human p-α-SYN ELISA Kit (AE90954Hu, AMEKO, Shanghai, China). High-sensitivity C-reactive protein (HsCRP), human albumin (ALB), human immunoglobulin G (IgG), and human retinol-binding protein 4 (RBP4) were measured with an ELISA kit (Elabscience Biotechnology, Wuhan, Hubei, China).

Uric acid (UA), total cholesterol (Chol), high-density lipoprotein cholesterol (HDL-C), low-density lipoprotein cholesterol (LDL-C), adenosine deaminase (ADA) activity, superoxide dismutase (SOD), lactate dehydrogenase (LDH) and glucose (GLU) were determined with colorimetric assay kits (Elabscience Biotechnology, Wuhan, Hubei, China).

Lymphocytes and neutrophils in peripheral blood were counted using the Sysmex XN-10 Hematology Analyzer (Sysmex Corporation, Kobe, Japan).

Fibrinogen (FIB), D-dimer (DDI), and plasminogen (PLG) were detected using the Clauss method with an STA compact coagulometer (Sysmex Corporation, Kobe, Japan).

MRI imaging and quantification of subtle blood–brain barrier permeability

Magnetic resonance imaging (MRI) images were scanned with 3.0 T Philips Ingenia. The dynamic contrast-enhancement magnetic resonance imaging (DCE-MRI) acquisition parameters included an 8° flip angle, 1.74/3.78 ms echo time/repetition time (TE/TR), 13.4 cm field of view (FOV), 140 × 140 in-plane matrix size, and 2-mm slice thickness with no gap. The T1-weighted MRI acquisition parameters included 90° flip angle, 20/2000 ms TE/TR, 12.9 × 9 cm^2 FOV, 292 × 208 in-plane matrix size, and 6-mm slice thickness. The SWI MRI acquisition parameters included a 15° flip angle, 20/29 ms TE/TR, 10.9 cm^2 FOV, 244 × 242 in-plane matrix size, and 2-mm slice thickness. Gadoterate meglumine (Dotarem®, Guerbet, France) (0.05 mmol/kg) was administered intravenously into the antecubital vein using a power injector at a rate of 3 mL/s followed by a 25 mL saline flush 30 s into the DCE scan. All MRI scans were performed in the Department of Radiology of Zhujiang Hospital of Southern Medical University. The MRI images were processed and analyzed by Brainnow Medical Technology Ltd. (Hong Kong, China). The region of interest (ROI) in the substantia nigra was segmented on the individual's SWI MRI image, and the corpus striatum was segmented on the T1W MRI image using atlas-based segmentation and transferred to the DCE-MRI image using rigid registration. K^{trans} statistics were calculated in the substantia nigra and corpus striatum ROIs with the methods proposed by Berislav V. Zlolovic[51]. The arterial input function (AIF), which was extracted from a region of interest (ROI) positioned at the internal carotid artery, was fitted with a biexponential function prior to fitting with Pk modeling (Pharmacokinetics Modeling). This method converts signal intensities to concentration values, which were used to calculate quantitative parameters and the K^{trans} map. The K^{trans} map is the volume transfer constant between blood plasma and the extracellular-extra vascular space (EES). Thus, the regional BBB K^{trans} permeability was measured on both sides of the substantia nigra and striatum. MRI technicians were blinded to the clinical information.

Statistical analyses

We performed all statistical analyses in R version 3.6.1. Statistical significance was set at 0.05 (two-sided).

Descriptive statistics are shown as the median (IQR) or mean (SD) for continuous variables and as frequencies or proportions for categorical variables. The distributions of baseline variables between the discovery and validation cohorts were compared using the Wilcoxon Mann–Whitney test (for continuous variables) or the chi-square test (for categorical variables). Fisher's exact test was used when any cell count was less than 5.

A Cox proportional hazards model using adaptive least absolute shrinkage and selection operator (LASSO) was applied in this study. Cox regression analyses were used to estimate the hazard ratios (HRs) or odds ratios (ORs). The prediction accuracy of the nomogram models was evaluated using two methods: discrimination and model calibration. The former was measured by Harrell's concordance index (C-index), and the latter was evaluated by calibration plots predicting the probability of the development of disability milestones at 12, 36, and 60 months versus the observed probability. Individual risk scores were obtained by applying the nomogram. An optimal cutoff point for the risk score was computed to stratify patients into low-risk and high-risk groups. Log-rank statistics were used to determine the optimal cutoff to provide the largest discrepancy between the low- and high-risk groups. The median (95% CI) cumulative risks of the first milestone were estimated using the Kaplan–Meier method. Differences in the cumulative risk of the first milestone between the discovery and validation cohorts were determined using the log-rank test.

Linear mixed-effects models (LMEMs) with visit time as a fixed effect were used to analyze the dynamic change in pFN among different clinical subtypes classified by the rate of disease progression (mild, aggressive, and N/A). A linear mixed-effects model was also used to relate the pFN rate of change to the H&Y stage and LED rate of change.

The Spearman correlation test and U-shape curve fitting were used to correlate the plasma FN level and plasma phosphorylated α-synuclein value.

Two independent samples nonparametric tests (Mann–Whitney test) were applied to compare the difference in the K^{trans} value between the low-pFN and high-pFN groups.

pFN was normally distributed after log transformation, as confirmed by Kolmogorov–Smirnov tests. Linear regression analysis was used to analyze the correlation between the concentration of the level of FN in plasma and cerebral spinal fluid (CSF), with age, sex, and disease duration as covariates.

Data availability

The data that support the findings of this study are available from the corresponding author, upon reasonable request. Shuzhen Zhu and Qing Wang have accessed and verified the data, and they were responsible for the decision to submit the manuscript.

Received: 10 July 2024; Accepted: 13 December 2024;
Published online: 02 January 2025

References

1. Parnetti, L. et al. CSF and blood biomarkers for Parkinson's disease. *Lancet Neurol.* **18**, 573–586 (2019).
2. Coelho, M. & Ferreira, J. J. Late-stage Parkinson disease. *Nat. Rev. Neurol.* **8**, 435–442 (2012).
3. Coelho, M. et al. Late-stage Parkinson's disease: the Barcelona and Lisbon cohort. *J. Neurol.* **257**, 1524–1532 (2010).

4. Hely, M. A., Morris, J. G., Reid, W. G. & Trafficante, R. Sydney multicenter study of Parkinson's disease: non-L-dopa-responsive problems dominate at 15 years. *Mov. Disord.* **20**, 190–199 (2005).
5. Hely, M. A., Reid, W. G., Adena, M. A., Halliday, G. M. & Morris, J. G. The Sydney multicenter study of Parkinson's disease: the inevitability of dementia at 20 years. *Mov. Disord.* **23**, 837–844 (2008).
6. Fabbri, M. et al. Personalized care in late-stage Parkinson's disease: challenges and opportunities. *J. Pers. Med.* **12**, 813 (2022).
7. Echebarria, S. G. Late-stage Parkinson's disease in the Lisbon-Barcelona cohorts: past phenomenology and today's clinical needs. *J. Neurol.* **258**, 918–919 (2011).
8. De Pablo-Fernandez, E., Lees, A. J., Holton, J. L. & Warner, T. T. Prognosis and neuropathologic correlation of clinical subtypes of Parkinson disease. *JAMA Neurol.* **76**, 470–479 (2019).
9. Zhang, J. et al. Longitudinal assessment of tau and amyloid beta in cerebrospinal fluid of Parkinson disease. *Acta Neuropathol.* **126**, 671–682 (2013).
10. Dadu, A. et al. Identification and prediction of Parkinson's disease subtypes and progression using machine learning in two cohorts. *NPJ Parkinson's Dis.* **8**, 172 (2022).
11. Sadaei, H. J. et al. Genetically-informed prediction of short-term Parkinson's disease progression. *NPJ Parkinson's Dis.* **8**, 143 (2022).
12. Wood, H. Parkinson disease: plasma alpha-synuclein - a potential marker of cognitive impairment in Parkinson disease. *Nat. Rev. Neurol.* **13**, 450 (2017).
13. Chahine, L. M. & Stern, M. B. Parkinson's disease biomarkers: where are we and where do we go next? *Mov. Disord. Clin. Pract.* **4**, 796–805 (2017).
14. Compta, Y. et al. Combined dementia-risk biomarkers in Parkinson's disease: a prospective longitudinal study. *Parkinsonism Relat. Disord.* **19**, 717–724 (2013).
15. Aarsland, D., Rajkumar, A. P. & Hye, A. Novel evidence associates higher plasma alpha-synuclein levels and cognitive impairment in Parkinson's disease. *J. Neurol. Neurosurg. Psychiatry* **88**, 808 (2017).
16. Wang, H. et al. Plasma alpha-synuclein and cognitive impairment in the Parkinson's associated risk syndrome: a pilot study. *Neurobiol. Dis.* **116**, 53–59 (2018).
17. Backstrom, D. C. et al. Cerebrospinal fluid patterns and the risk of future dementia in early, incident Parkinson disease. *JAMA Neurol.* **72**, 1175–1182 (2015).
18. Parnetti, L. et al. Cerebrospinal fluid lysosomal enzymes and alpha-synuclein in Parkinson's disease. *Mov. Disord.* **29**, 1019–1027 (2014).
19. Gustafson, D. R., Skoog, I., Rosengren, L., Zetterberg, H. & Blennow, K. Cerebrospinal fluid beta-amyloid 1-42 concentration may predict cognitive decline in older women. *J. Neurol. Neurosurg. Psychiatry* **78**, 461–464 (2007).
20. Schrag, A., Siddiqui, U. F., Anastasiou, Z., Weintraub, D. & Schott, J. M. Clinical variables and biomarkers in prediction of cognitive impairment in patients with newly diagnosed Parkinson's disease: a cohort study. *Lancet Neurol.* **16**, 66–75 (2017).
21. Majbour, N. K. et al. Longitudinal changes in CSF alpha-synuclein species reflect Parkinson's disease progression. *Mov. Disord.* **31**, 1535–1542 (2016).
22. Munoz-Delgado, L. et al. Peripheral inflammation is associated with dopaminergic degeneration in Parkinson's disease. *Mov. Disord.* **38**, 755–763 (2023).
23. Yacoubian, T. A. et al. Brain and systemic inflammation in de novo Parkinson's disease. *Mov. Disord.* **38**, 743–754 (2023).
24. Bartl, M. et al. Blood markers of inflammation, neurodegeneration, and cardiovascular risk in early Parkinson's disease. *Mov. Disord.* **38**, 68–81 (2023).
25. Kempster, P. A., O'Sullivan, S. S., Holton, J. L., Revesz, T. & Lees, A. J. Relationships between age and late progression of Parkinson's disease: a clinico-pathological study. *Brain* **133**, 1755–1762 (2010).
26. Postuma, R. B. et al. MDS clinical diagnostic criteria for Parkinson's disease. *Mov. Disord.* **30**, 1591–1601 (2015).
27. Griffanti, L. et al. Cohort profile: the Oxford Parkinson's Disease Centre Discovery Cohort MRI substudy (OPDC-MRI). *BMJ Open* **10**, e034110 (2020).
28. Thi Lai, T. et al. Microglial inhibition alleviates alpha-synuclein propagation and neurodegeneration in Parkinson's disease mouse model. *NPJ Parkinson's Dis.* **10**, 32 (2024).
29. Shin, C. et al. Diagnostic accuracy and predictors of alpha-synuclein accumulation in the gastrointestinal tract of Parkinson's disease. *NPJ Parkinson's Dis.* **10**, 155 (2024).
30. Huang, X., Hussain, B. & Chang, J. Peripheral inflammation and blood-brain barrier disruption: effects and mechanisms. *CNS Neurosci. Therapeut.* **27**, 36–47 (2021).
31. von Herrmann, K. M. et al. NLRP3 expression in mesencephalic neurons and characterization of a rare NLRP3 polymorphism associated with decreased risk of Parkinson's disease. *NPJ Parkinson's Dis.* **4**, 24 (2018).
32. Munoz-Delgado, L. et al. Peripheral inflammatory immune response differs among sporadic and familial Parkinson's disease. *NPJ Parkinson's Dis.* **9**, 12 (2023).
33. Lyra, P. et al. Self-reported periodontitis and C-reactive protein in Parkinson's disease: a cross-sectional study of two American cohorts. *NPJ Parkinson's Dis.* **8**, 40 (2022).
34. Romano, S. et al. Meta-analysis of the Parkinson's disease gut microbiome suggests alterations linked to intestinal inflammation. *NPJ Parkinson's Dis.* **7**, 27 (2021).
35. Metzger, J. M. et al. In vivo imaging of inflammation and oxidative stress in a nonhuman primate model of cardiac sympathetic neurodegeneration. *NPJ Parkinson's Dis.* **4**, 22 (2018).
36. Houser, M. C. & Tansey, M. G. The gut-brain axis: is intestinal inflammation a silent driver of Parkinson's disease pathogenesis? *NPJ Parkinson's Dis.* **3**, 3 (2017).
37. Grigoletto, J. et al. Velusetrag rescues GI dysfunction, gut inflammation and dysbiosis in a mouse model of Parkinson's disease. *NPJ Parkinson's Dis.* **9**, 140 (2023).
38. Ton, T. G. et al. Markers of inflammation in prevalent and incident Parkinson's disease in the Cardiovascular Health Study. *Parkinsonism Relat. Disord.* **18**, 274–278 (2012).
39. Yang, W. et al. Contra-directional expression of plasma superoxide dismutase with lipoprotein cholesterol and high-sensitivity C-reactive protein as important markers of Parkinson's disease severity. *Front. Aging Neurosci.* **12**, 53 (2020).
40. Shen, J. et al. Plasma MIA, CRP, and albumin predict cognitive decline in Parkinson's disease. *Ann. Neurol.* **92**, 255–269 (2022).
41. Athauda, D. et al. The impact of type 2 diabetes in Parkinson's disease. *Mov. Disord.* **37**, 1612–1623 (2022).
42. Simon, K. C. et al. Mendelian randomization of serum urate and Parkinson disease progression. *Ann. Neurol.* **76**, 862–868 (2014).
43. Stecher, V. J., Kaplan, J. E., Connolly, K., Mielens, Z. & Saelens, J. K. Fibronectin in acute and chronic inflammation. *Arthritis Rheum.* **29**, 394–399 (1986).
44. Lemanska-Perek, A. & Adamik, B. Fibronectin and its soluble EDA-FN isoform as biomarkers for inflammation and sepsis. *Adv. Clin. Exp. Med.* **28**, 1561–1567 (2019).
45. Lemanska-Perek, A., Krzyzanowska-Golab, D., Skalec, T. & Adamik, B. Plasma and cellular forms of fibronectin as prognostic markers in sepsis. *Mediat. Inflamm.* **2020**, 8364247 (2020).
46. Pott, G., Lohmann, J., Zundorf, P. & Gerlach, U. [Reduced plasma fibronectin in patients with sepsis and shock (author's transl)]. *Dtsch. Medizinische Wochenschr.* **106**, 532–534 (1981).
47. Nagelschmidt, M., Rink, A. D. & Neugebauer, E. Plasma concentration of biologically active fibronectin and fibronectin bound to gelatin-like material in a porcine model of hyperdynamic endotoxic shock. *Shock* **14**, 484–489 (2000).

48. Duan, W. M. et al. Enhancement of nigral graft survival in rat brain with the systemic administration of synthetic fibronectin peptide V. *Neuroscience* **100**, 521–530 (2000).
49. Tonge, D. A. et al. Fibronectin supports neurite outgrowth and axonal regeneration of adult brain neurons in vitro. *Brain Res.* **1453**, 8–16 (2012).
50. Dai, W. et al. Brain delivery of fibronectin through bioactive phosphorous dendrimers for Parkinson's disease treatment via cooperative modulation of microglia. *Bioact. Mater.* **38**, 45–54 (2024).
51. Nation, D. A. et al. Blood-brain barrier breakdown is an early biomarker of human cognitive dysfunction. *Nat. Med.* **25**, 270–276 (2019).

Acknowledgements

This work was supported by the National Natural Science Foundation of China (NO: U24A20694, 82071414, 82471433), Initiated Foundation of Zhujiang Hospital (NO: 02020318005), Scientific Research Foundation of Guangzhou (NO: 202206010005) and Science and Technology Program of Guangdong of China (NO: 2020A0505100037) to Q.W; and National Research Foundation Singapore to EK; and the National Natural Science Foundation of China (NO: 82171253) and Science and Technology Program of Guangdong of China (NO: 2022A1515010522) to S.Z.Z. The funders of the study had no role in study design, data collection, data analysis, data interpretation, or writing of the report. Shuzhen Zhu and Qing Wang had full access to all the data in the study and had final responsibility for the decision to submit for publication. We thank all participants and their family members for taking part in this study. We additionally thank Haifan Gong for polishing the manuscript. We would like to thank Wenjie Zhang for arranging a portion of the clinical documents.

Author contributions

Conceived and designed the study: S.Z.Z., H.L.L., Y.H.Z., E.K.T., and Q.W. Performed the study: S.Z.Z., Z.F.H., J.M.H., G.X.L., S.J.Y., Z.H.C., S.H.C., Y.R.L., W.B.X., and Q.W. Critically reviewed or revised the manuscript for important intellectual content: M.Y.L., Y.P., Z.C.X., R.F.Q., L.S., H.Z., M.Z.L., F.H.H., L.B., L.L.C., C.D., E.K.T., and K.R.C. Data statistics and analysis: S.Z.Z., C.W.Y., X.B.W., C.D., and Q.W. Wrote the paper: S.Z.Z., K.R.C., E.K.T., and Q.W. K.R.C., E.K.T., and K.P.D. acted as advisors to inclusion and exclusion criteria. All authors reviewed the interim drafts and the final version of the manuscript, and agree with its content and submission. S.Z.Z. and Q.W. had final responsibility for the decision to submit this manuscript for publication.

Competing interests

The authors declare no competing interests.

Additional information

Supplementary information The online version contains supplementary material available at https://doi.org/10.1038/s41531-024-00865-1.

Correspondence and requests for materials should be addressed to K. Ray Chaudhuri, Eng-King Tan or Qing Wang.